BJ www.biochemj.org

Biochem. J. (2010) **429**, 485–495 (Printed in Great Britain) doi:10.1042/BJ20091956





# Calcium- and polyphosphate-containing acidic granules of sea urchin eggs are similar to acidocalcisomes, but are not the targets for NAADP

Isabela B. RAMOS*†, Kildare MIRANDA†‡, Douglas A. PACE*, Katherine C. VERBIST*, Fu-Yang LIN§, Yonghui ZHANG‖, Eric OLDFIELD§‖, Ednildo A. MACHADO†‡, Wanderley DE SOUZA† and Roberto DOCAMPO*[1]

*Department of Cellular Biology and Center for Tropical and Emerging Global Diseases, University of Georgia, Athens, GA 30602, U.S.A., †Instituto de Biofísica Carlos Chagas Filho, and Instituto Nacional de Ciência e Tecnologia em Bioimagens e Biologia Estrutural, Universidade Federal do Rio de Janeiro, Rio de Janeiro, RJ 21941, Brazil, ‡Instituto Nacional de Metrologia Normalização e Qualidade Industrial, Diretoria de Programas, Xerém, Rio de Janeiro, RJ 25250, Brazil, §Center for Biophysics and Computational Biology, University of Illinois at Urbana-Champaign, Urbana, IL 61801, U.S.A., and ‖Department of Chemistry, University of Illinois at Urbana-Champaign, Urbana, IL 61801, U.S.A.

Acidocalcisomes are acidic calcium-storage compartments described from bacteria to humans and characterized by their high content in poly P (polyphosphate), a linear polymer of many tens to hundreds of $P_i$ residues linked by high-energy phosphoanhydride bonds. In the present paper we report that millimolar levels of short-chain poly P (in terms of $P_i$ residues) and inorganic $PP_i$ are present in sea urchin extracts as detected using $^{31}$P-NMR, enzymatic determinations and agarose gel electrophoresis. Poly P was localized to granules randomly distributed in the sea urchin eggs, as shown by labelling with the poly-P-binding domain of *Escherichia coli* exopolyphosphatase. These granules were enriched using iodixanol centrifugation and shown to be acidic and to contain poly P, as determined by Acridine Orange and DAPI (4′,6′-diamidino-2-phenylindole) staining respectively. These granules also contained large amounts of calcium, sodium, magnesium, potassium and zinc, as detected by X-ray microanalysis, and bafilomycin $A_1$-sensitive ATPase, pyrophosphatase and exopolyphosphatase activities, as well as $Ca^{2+}/H^+$ and $Na^+/H^+$ exchange activities, being therefore similar to acidocalcisomes described in other organisms. Calcium release from these granules induced by nigericin was associated with poly P hydrolysis. Although NAADP (nicotinic acid–adenine dinucleotide phosphate) released calcium from the granule fraction, this activity was not significantly enriched as compared with the NAADP-stimulated calcium release from homogenates and was not accompanied by poly P hydrolysis. GPN (glycyl-L-phenylalanine-naphthylamide) released calcium when added to sea urchin homogenates, but was unable to release calcium from acidocalcisome-enriched fractions, suggesting that these acidic stores are not the targets for NAADP.

Key words: acidocalcisome, calcium, glycyl-L-phenylalanine-naphthylamide (GPN), polyphosphate, sea urchin egg, vacuolar $H^+$-ATPase.

## INTRODUCTION

The sea urchin egg has been an invaluable model for studying $Ca^{2+}$ homoeostasis and signalling. Intracellular $Ca^{2+}$ increases upon fertilization and is important for the generation of the fertilization envelope and for initiation of the biochemical events that serve to wake the egg from a state of dormancy [1].

A number of second messengers able to release $Ca^{2+}$ from different intracellular stores were described for the first time in sea urchin eggs, such as cADPR (cyclic adenosine diphosphate ribose) [2] and NAADP (nicotinic acid–adenine dinucleotide phosphate) [3]. Whereas cADPR and $IP_3$ (inositol 1,4,5-trisphosphate) release $Ca^{2+}$ from the ER (endoplasmic reticulum) of sea urchin eggs, NAADP does it from acidic vesicles that were proposed to be lysosome-like organelles [4], possibly the so-called yolk platelets [5]. NAADP was also shown to increase the pH of these acidic vesicles by a mechanism coupled to $Ca^{2+}$ release via the NAADP receptor [6]. It was proposed that the fall in the luminal $[Ca^{2+}]$ allows $H^+$ to bind to vacated sites on a luminal polyanionic matrix, thus resulting in alkalinization of the store [6].

The findings that NAADP released $Ca^{2+}$ from acidic organelles of sea urchin eggs [4] led to investigations as to whether NAADP was also able to mobilize $Ca^{2+}$ from lysosomes of mammalian cells. NAADP was shown initially to release $Ca^{2+}$ from acidic organelles of pancreatic acinar and $\beta$-cells [7,8], coronary artery myocytes [9] and the phaeochromocytoma cell line PC12 [10], but apparently not from T-lymphocyte cell lines [11,12]. It was found that NAADP-induced $Ca^{2+}$ release was associated with endolysosomal function because the $Ca^{2+}$-release response was dependent on a proton gradient maintained by an ATP-dependent vacuolar-type proton pump that is primarily present in the endocytic pathway [13]. Accumulating evidence showed that this NAADP-sensitive $Ca^{2+}$ store was unique and distinct from $IP_3$- and cADPR-sensitive $Ca^{2+}$ stores [14,15], and results suggested that, at least in rat liver, it is the lysosome [13]. Two-pore channels have recently emerged as potential receptors for NAADP in the lysosomes of mammalian cells [16–18], and they have now been identified as NAADP targets for $Ca^{2+}$ release in the sea urchin [19].

Sea urchin eggs have a number of intracellular vesicles and several types of granules in their cytoplasm, as identified by electron microscopy. Among them are the cortical granules, which are located close to the surface and are exocytosed upon fertilization and formation of the fertilization envelope, the yolk platelets, which are an abundant group of organelles of high

Abbreviations used: ASW, artificial sea water; cADPR, cyclic adenosine diphosphate ribose; DAPI, 4′,6′-diamidino-2-phenylindole; ER, endoplasmic reticulum; GluIM, gluconate intracellular-like medium; GPN, glycyl-L-phenylalanine-naphthylamide; $IP_3$, inositol 1,4,5-trisphosphate; LC, long-chain; NAADP, nicotinic acid–adenine dinucleotide phosphate; poly P, polyphosphate; PPase, pyrophosphatase; PPBD, poly-P-binding domain; PPX, exopolyphosphatase; rPPX1, recombinant *Saccharomyces cerevisiae* PPX1; SC, short-chain; TBS, Tris-buffered saline.

[1] To whom correspondence should be addressed (email rdocampo@uga.edu).

and uniform electron-density and that can occupy approximately half the volume of the egg [20], and the clear granules [21,22] characterized by their clear appearance, that are distributed at random in the unfertilized eggs [21]. Both the cortical granules [4] and the clear granules [21] are acidic, whereas the yolk platelets increase their acidity from pH 6.8 to pH 6.1 upon fertilization [23]. These changes in pH in yolk platelets (alkalinization on NAADP stimulation and acidification upon fertilization) reveals the multiphasic nature of this phenomenon, with the NAADP-induced response being a 'rapid' response and acidification upon fertilization being a 'slow' response.

Yolk platelets have been proposed to be the acidic organelles responsible for $Ca^{2+}$ release upon NAADP stimulation [4,5]. This is in agreement with experiments using eggs stratified by centrifugation. Under these conditions, yolk platelets localize to the centrifugal pole, which is the site where the higher $Ca^{2+}$ release occurs upon local photolysis of caged NAADP [24] and is opposite to the nucleus and lipid droplets. However, photolysis of NAADP at the centripetal pole, which is the region where clear granules localize, also results in a transient $Ca^{2+}$ release [24]. Interestingly this region of clear granules is the one more intensely labelled with Acridine Orange [21], suggesting that clear granules are more acidic than yolk platelets. In contrast LysoTracker Red appears to preferentially label the yolk platelets [4] and this labelling disappears after treatment with GPN (glycyl-L-phenylalanine-naphthylamide), a substrate of the lysosomal cathepsin C that selectively disrupts these organelles via osmotic lysis [25]. Interestingly, although yolk platelets are distributed at random in the sea urchin egg, NAADP induces a peripheral vesicular alkalinization, even when injected into the middle of the egg, suggesting the presence of a subpopulation of NAADP-sensitive stores [6].

The clear granules of sea urchin eggs are morphologically very similar to acidocalcisomes, which are lysosome-related organelles characterized by their abundant content of the polyanion poly P (polyphosphate) bound to cations such as calcium, magnesium and zinc [26]. Acidocalcisomes are present in trypanosomatid and apicomplexan parasites [26], as well as in the green alga *Chlamydomonas reinhardtii* [27] and the slime mould *Dictyostelium discoideum* [28], and were also identified in bacteria [29,30], human platelets [31], and insect [32] and chicken [33] eggs. As acidocalcisomes are acidic, rich in $Ca^{2+}$ and in the polyanion poly P, and it has been shown that $Ca^{2+}$ can be released from them after their alkalinization with $NH_4Cl$ or by the $K^+/H^+$ ionophore nigericin [34], we investigated whether some of the acidic granules of sea urchin eggs are equivalent to acidocalcisomes, and whether they are also targets for NAADP-stimulated $Ca^{2+}$ release.

## MATERIALS AND METHODS

### Chemicals and reagents

ATP, nigericin, valinomycin, DAPI (4′,6-diamidino-2-phenylindole), $IP_3$, NAADP, $PP_i$, tripolyphosphate (poly $P_3$), poly $P_{75+}$ and protease inhibitors (P8340) were purchased from Sigma Chemical. Coomassie Blue protein assay reagent was from Bio-Rad Laboratories. The anti-Xpress epitope monoclonal antibody and Fluo-3 were from Invitrogen. Bafilomycin $A_1$ was from Kamiya Biomedical. *Escherichia coli* strain CA38 pTrcPPX1 was kindly provided by Professor Arthur Kornberg (Stanford University School of Medicine, Stanford, CA, U.S.A.). *E. coli* DH5a harbouring pTrc-PPBD was provided by Dr Katsuharu Saito (Shinshu University, Nagano-Ken, Japan). LysoTracker Red DND-99 was from Invitrogen. All other reagents were of analytical grade.

### Egg collection and homogenate preparation

Sea urchins were obtained from Gulf Specimen Marine Laboratories or from the Guanabara Bay (Rio de Janeiro, Brazil). Eggs from *Lytechinus variegatus* or *Arbacia punctulata* were harvested by intracoelomic injection of 0.5 M KCl and collected in ASW (artificial sea water; 435 mM NaCl, 40 mM $MgCl_2$, 15 mM $MgSO_4$, 11 mM $CaCl_2$, 10 mM KCl, 2.5 mM $NaHCO_3$ and 20 mM Tris base, pH 8.0). Egg homogenates were prepared as described previously [6]. Briefly, eggs were washed four times in $Ca^{2+}$-free ASW (the first two washes containing 1 mM EGTA) and then washed in GluIM (gluconate intracellular-like medium; 250 mM potassium gluconate, 250 mM *N*-methylglucamine, 20 mM Hepes and 1 mM $MgCl_2$, pH 7.2) without an ATP-generating system. Eggs were then homogenized in the same medium in the presence of protease inhibitors (P8340, Sigma). The homogenate (50 %, v/v) was centrifuged at 13000 ***g*** for 10 s at 4 °C, and the supernatant was sequentially diluted in equal volumes of GluIM over a period of 3 h, as described previously [6]. Microscopy experiments were performed with both species of sea urchin eggs with similar results. All other experiments were performed using *L. variegatus* eggs.

### Isolation of dense granules

The egg homogenate (8 ml, $\sim 4 \times 10^5$ eggs/ml) was centrifuged at 5000 ***g*** for 10 min at 4 °C. The supernatant (4 ml) was then loaded on to the top of a 20 % iodixanol fractionation medium (OptiPrep™, Greiner Bio-One) diluted in GluIM buffer (20 ml). The preparation was centrifuged at 60000 ***g*** for 60 min at 4 °C. The pellet was resuspended in 100 $\mu$l of GluIM buffer, washed at least three times in GluIM, and used as the dense granule fraction.

### Electron microscopy and X-ray microanalysis

For imaging, whole cells and dense granule fractions were washed first in 100 mM Hepes buffer (pH 7.4) and directly applied to Formvar-coated 200-mesh copper grids, allowed to adhere for 10 min at room temperature (22 °C), blotted dry and observed directly in an energy-filtering Zeiss 902 transmission electron microscope. This treatment avoided salt precipitation. Electron energy-filtered images were taken at an energy loss of 70 eV using a spectrometer slit width of 10 eV. For X-ray microanalysis, samples were examined in a JEOL 1200 EX transmission electron microscope. X-rays were collected for 150 s using a Si (Li) detector with a Norvar window on a 0–10 KeV energy range with a resolution of 10 eV/channel. Analysis was performed using a Noran Voyager III analyser with a standard analysis identification program. No changes in the size of the organelles were detected when the fractions were suspended in 100 mM Hepes (pH 7.4), plus 300 mM or 400 mM sucrose, instead of 100 mM Hepes alone.

For conventional electron microscopy, eggs and dense granule fractions were fixed in 4 % formaldehyde and 2.5 % glutaraldehyde diluted in 0.1 M sodium cacodylate buffer (pH 7.3) at 4 °C for 24 h, and then embedded in epoxy resin, sectioned and stained using standard methods. To verify that osmotic conditions did not change the size of organelles, the fixative was also diluted in ASW, but no changes in the morphology of different organelles were observed.

### Extraction of $PP_i$ and long- and short-chain poly P

Egg homogenates were centrifuged at 16000 ***g*** for 30 min at 4 °C and the pellet was treated with methods to extract either LC (long-chain) or SC (short-chain) poly P and $PP_i$. Different samples were used for each method. Aliquots of known volumes from different steps of the dense granule fraction separation were also obtained and centrifuged at 14000 ***g*** for 30 min at 4 °C. The pellets were extracted and used for poly P and $PP_i$ determinations. LC poly P extraction was performed as described by Ault-Riché et al. [35]. SC poly P and $PP_i$ extraction was performed as described by Ruiz et al. [34]. Protein measurements were performed using the Bradford protein assay kit (Bio-Rad Laboratories).

### Analysis of $PP_i$ and poly P

Poly P levels were determined from the amount of $P_i$ released upon treatment with an excess of rPPX1 [recombinant *Saccharomyces cerevisiae* PPX (exopolyphosphatase) 1]. The recombinant enzyme was prepared as described previously [34]. Aliquots of LC and SC poly P extracts (always less than 1.5 nmol) were incubated for 15 min at 37 °C with 60 mM Tris/HCl (pH 7.5), 6.0 mM $MgCl_2$ and 3000–5000 units of purified rPPX1 in a final volume of 100 $\mu$l. One unit corresponds to the release of 1 pmol of $P_i$/min at 35 °C. Release of $P_i$ was monitored using the method of Lanzetta et al. [36]. For $PP_i$ quantification, the procedure was essentially the same, but using an excess of soluble TiPPase [thermostable inorganic PPase (pyrophosphatase); New England Biolabs], 0.04 unit per reaction, in 50 mM Tris/HCl (pH 7.5) and 5 mM $MgCl_2$, for 30 min at 35 °C. To detect poly P degradation by dense granule fractions in the presence of 10 $\mu$M nigericin, aliquots were collected after 5, 10 and 15 min and centrifuged at 14000 ***g*** for 10 s, and the pellets were used for poly P extraction and determinations, as described above. The intracellular concentration of phosphate compounds was calculated taking into account a volume of 904 pl/egg.

### NMR spectroscopy

For NMR analyses, EDTA was added to poly P extracts to a final concentration of 25 mM prior to adjusting to pH 7.0. All of the extracts contained 10 % (v/v) $^2H_2O$ to provide a field-frequency lock. Phosphorus NMR spectra were acquired at 242.8 MHz using a Varian INOVA NMR spectrometer equipped with a 14.1 T Oxford Instruments magnet. For perchloric acid extracts, 10784 transients were collected at room temperature using 25 $\mu$s (90°) pulse excitation, a 20-kHz spectral width, 32768 data points and a 5 s recycle time. Inverse gated proton decoupling was used to remove NOE (nuclear Overhauser effect) and J-coupling effects. The chemical shifts of all the $^{31}P$ spectra were referenced to 0 p.p.m. using an 85 % phosphoric acid external standard. The specific assignments of individual resonances were based on published chemical shifts and $^{31}P$–$^{31}P$ scalar couplings and, in some cases, co-addition of authentic compounds. NMR spectra were processed using the MacNuts 0.9.4 program (Acorn NMR) and included base-line correction, zero-filling and a 2-Hz exponential line broadening prior to Fourier transformation.

### Fluorescence microscopy

For poly P localization in whole eggs, the recombinant PPBD (poly-P-binding domain) of *E. coli* PPX linked to an Xpress epitope tag was used, as described previously [37]. Briefly, eggs suspended in ASW were permeabilized with 0.1 % Triton X-100 for 2 min. After washing in TBS [Tris-buffered saline; 100 mM Tris/HCl (pH 7.2) and 150 mM NaCl], eggs were incubated in blocking buffer (3 % BSA in TBS, pH 7.2) for 30 min. PPBD (8 $\mu$g/ml) and 10 $\mu$g/ml anti-Xpress epitope monoclonal antibody were added, and the samples were incubated for 1 h under gentle agitation. The samples were washed with blocking buffer and TBS, and fixed in 4 % paraformaldehyde diluted in TBS for 30 min. After fixation the eggs were blocked for 15 min in 100 mM $NH_4Cl$ in TBS, and for an additional 30 min in blocking buffer plus 0.1 % Tween 20. Secondary antibodies (Alexa Fluor® 488-conjugated goat anti-mouse IgG; Invitrogen) were diluted in the same buffer (1:1000) and incubated with the eggs for 1 h under gentle agitation. After washing in blocking buffer plus Tween 20, the samples were observed using an Olympus IX-71 fluorescence microscope with a Photometrix $CoolSnap_{HQ}$ CCD (charge-coupled device) camera driven by Delta Vision software (Applied Precision) using filters with excitation at 480–500 nm and emission at 510–550 nm. For the egg three-dimensional projection (Supplementary Movie S1 at http://www.BiochemJ.org/bj/429/bj4290485add.htm), *z*-stacks were acquired and reconstructed using the same software as described above.

For localization of Acridine Orange and DAPI, the dense granule fraction was incubated with 3 $\mu$M Acridine Orange or 10 $\mu$g/ml DAPI for 10 min at room temperature in the presence of protease inhibitor cocktail (Sigma, P8340), 2 $\mu$g/ml oligomycin and 2 $\mu$g/ ml antimycin, and observed in the microscope described above with excitation at 340–380 nm for DAPI and at 450–490 nm for Acridine Orange, and emission >500 nm for both dyes.

### Egg stratification

Egg stratification was performed as reported previously [4,24]. PPBD and DAPI staining were performed as described above. For LysoTracker staining, eggs were incubated with 0.5 nM LysoTracker Red DND-99 for 30 min at room temperature before stratification [4], and then stained with PPBD as described above.

### Fluorimetry

$H^+$ movements, and $Ca^{2+}$ release were monitored using a fluorimeter (F4500, Hitachi Instruments). $H^+$ movements were monitored by following changes in Acridine Orange (6 $\mu$M) fluorescence (excitation at 495 nm, emission at 530 nm) after incubating dense granule fractions (50–80 $\mu$g of protein for bafilomycin experiments; 600–800 $\mu$g of protein for $Na^+/H^+$ and $Ca^{2+}/H^+$ experiments) in 2 ml of GluIM containing 2 $\mu$g/ml oligomycin and 2 $\mu$g/ml antimycin A. Acridine Orange was allowed to equilibrate for 2–5 min, whereas the dye partitioned into dense granules, and then valinomycin (10 $\mu$M), bafilomycin $A_1$ (1 $\mu$M) and/or nigericin (5 $\mu$M) were added as indicated. $Ca^{2+}$ release was measured following changes in the fluorescence (excitation 506 nm, emission 526 nm) of Fluo-3 (3 $\mu$M). Total homogenates and dense granule fractions (310 $\mu$g of protein for NAADP experiments; 600–800 $\mu$g of protein for GPN experiments) were diluted in 2 ml of GluIM buffer. $IP_3$ (300 nM), NAADP (200 nM) and nigericin (5 $\mu$M) were added where indicated in the Figures.

### Gel electrophoresis

Perchloric acid extracts were dried in a SpeedVac and resuspended in 60 mM Tris/HCl (pH 7.5) and 6.0 mM $MgCl_2$. For PPX-treated

samples, rPPX1 [34] was added (3000–5000 units) in a final volume of 50 $\mu$l and incubated for 30 min at 35 °C. Poly P samples were then mixed with DNA-loading buffer [10 mM Tris/HCl (pH 7.5), 10 mM EDTA, 0.25 % Orange-G and 0.65 % sucrose] and loaded into 1–2 % agarose gels. The gels were run at 200 V in TAE buffer [40 mM Tris/acetate (pH 8.2) and 1 mM EDTA] until the dye (Orange-G) reached the middle of the gel. The gels were then stained with 0.1 % Toluidine Blue for 1 h, and then de-stained with several changes of deionized water for 4 h.

### PPX and PPase activities in the dense granule fraction

Dense granule fractions were homogenized using a Teflon pestle tissue homogenizer in ice-cold reaction buffer for PPX [20 mM Tris/HCl, 5 mM magnesium acetate and 100 mM ammonium acetate (pH 7.5)], or PPase [50 mM Tris/HCl and 5 mM $MgCl_2$ (pH 7.5)] activities, and supplemented with protease inhibitor cocktail (P8340, Sigma). To these samples, 0.1 mM poly $P_{75+}$ or 0.1 $\mu$M $PP_i$ was added and aliquots were collected at 5, 10 and 15 min after substrate addition. The aliquots were centrifuged at 14 000 ***g*** for 10 s, and the pellets were processed for poly P and $PP_i$ determinations as described before. Controls were performed with no sample, incubating the substrates in plain buffer under the same conditions.

### Data analysis

All results are expressed as means $\pm$ S.D. or, when appropriate, S.E.M. for $n$ different experiments. Statistical significance was determined using a Student's $t$ test or by one-way ANOVA at $P<0.05$.

## RESULTS

### Ultrastructure and elemental analysis of sea urchin egg granules

Ultrastructural analysis of sea urchin eggs allowed the identification of several granules. The cortical granules (whose size varies from $0.39 \pm 0.02$ to $0.92 \pm 0.05$ $\mu$m diameter in different sea urchin species [38]) are located close to the surface and are identified by the presence of star-like dense material in their interior (Figure 1A, cg, thin arrow). An abundant group of organelles of approx. 1–2 $\mu$m diameter, oval form and high and uniform electron-density are known as yolk platelets (Figures 1B and 1C; YP) [20]. In addition, clear granules [21,22], characterized by their clear appearance and the presence in most of them of an electron-dense material in various states of condensation (Figures 1A and 1B, thick arrows), are distributed at random in the unfertilized eggs [20]. These clear granules, of an average diameter of $0.83 \pm 0.29$ $\mu$m, are very similar in their appearance to the acidocalcisomes described in different organisms [26]. A large number of other clear granules that are smaller (average diameter $0.19 \pm 0.04$ $\mu$m) than the granules described above, but which also have a similar appearance to acidocalcisomes (empty appearance with a thin-layer of dense material that sticks to the inner face of the membrane; Figures 1B and 1E, white arrowheads) and mitochondria (Figures 1B and 1D, black arrowheads) are also visible.

To investigate whether the clear granules correspond to acidocalcisomes, whole-cell mounts of sea urchin eggs or homogenates were analysed by energy-filtering transmission electron microscopy. Using this technique, the contrast of a given structure in the image solely arises from its mass density since these preparations are not stained. Many electron-dense vesicles

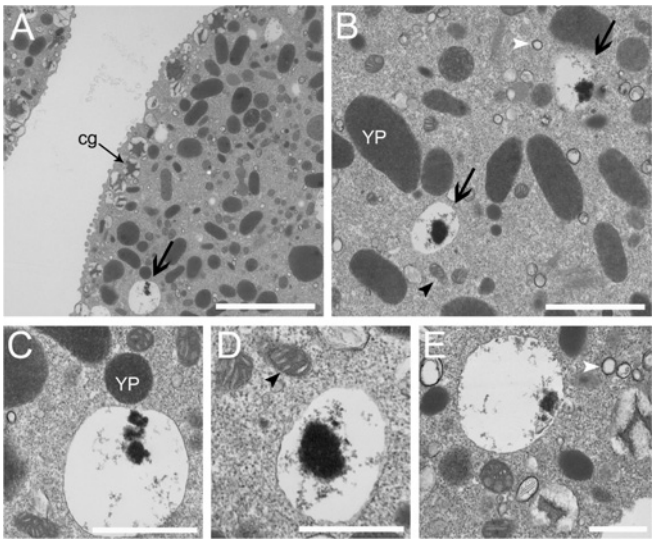


**Figure 1 Transmission electron microscopy of *A. punctulata* eggs**

The preparation was fixed and processed for standard electron microscopy. Cortical granules (cg, thin arrow), yolk platelets (YP) and 'clear granules' containing residual electron-dense material (thick arrow), smaller clear vesicles (white arrowheads) and mitochondria (black arrowheads) are indicated. Scale bars in (**A**) are 3 $\mu$m, (**B**) 1 $\mu$m and (**C**–**E**) 0.5 $\mu$m.

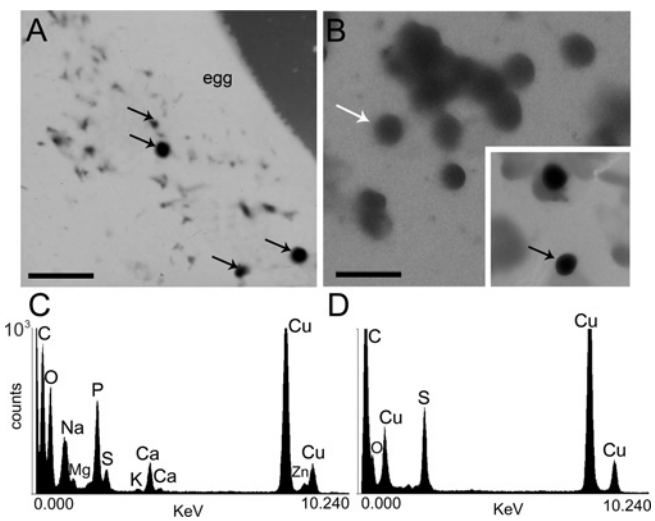


**Figure 2 Electron microscopy and X-ray microanalysis of whole intact eggs and homogenates**

(**A** and **B**) Electron energy-filtered transmission electron microscopy of an unfixed and unstained egg (**A**) or an egg homogenate (**B**) from *A. punctulata*. Dense granules are identified by black arrows. (**C**) Typical X-ray microanalysis spectrum of dense granules found in egg homogenates [black arrow in (**B**)]. (**D**) Typical X-ray microanalysis spectrum of a less-electron-dense vesicle (probably a yolk platelet) [white arrow in (**B**)] found in egg homogenates. Scale bars in (**A**) and (**B**) are 3 $\mu$m.

of various diameter (average $0.73 \pm 0.09$ $\mu$m) were seen in intact eggs (Figure 2A, black arrows) or homogenates (Figure 2B, black arrow). Other larger and less electron-dense vesicles (probably yolk platelets) were also observed (Figure 2B, white arrow). X-ray microanalysis of these vesicles was performed (Figures 2C and 2D). All ten spectra of the very-electron-dense vesicles taken from different homogenates were qualitatively similar showing considerable amounts of oxygen, sodium, magnesium, phosphorus, sulfur, calcium and zinc concentrated in their matrix

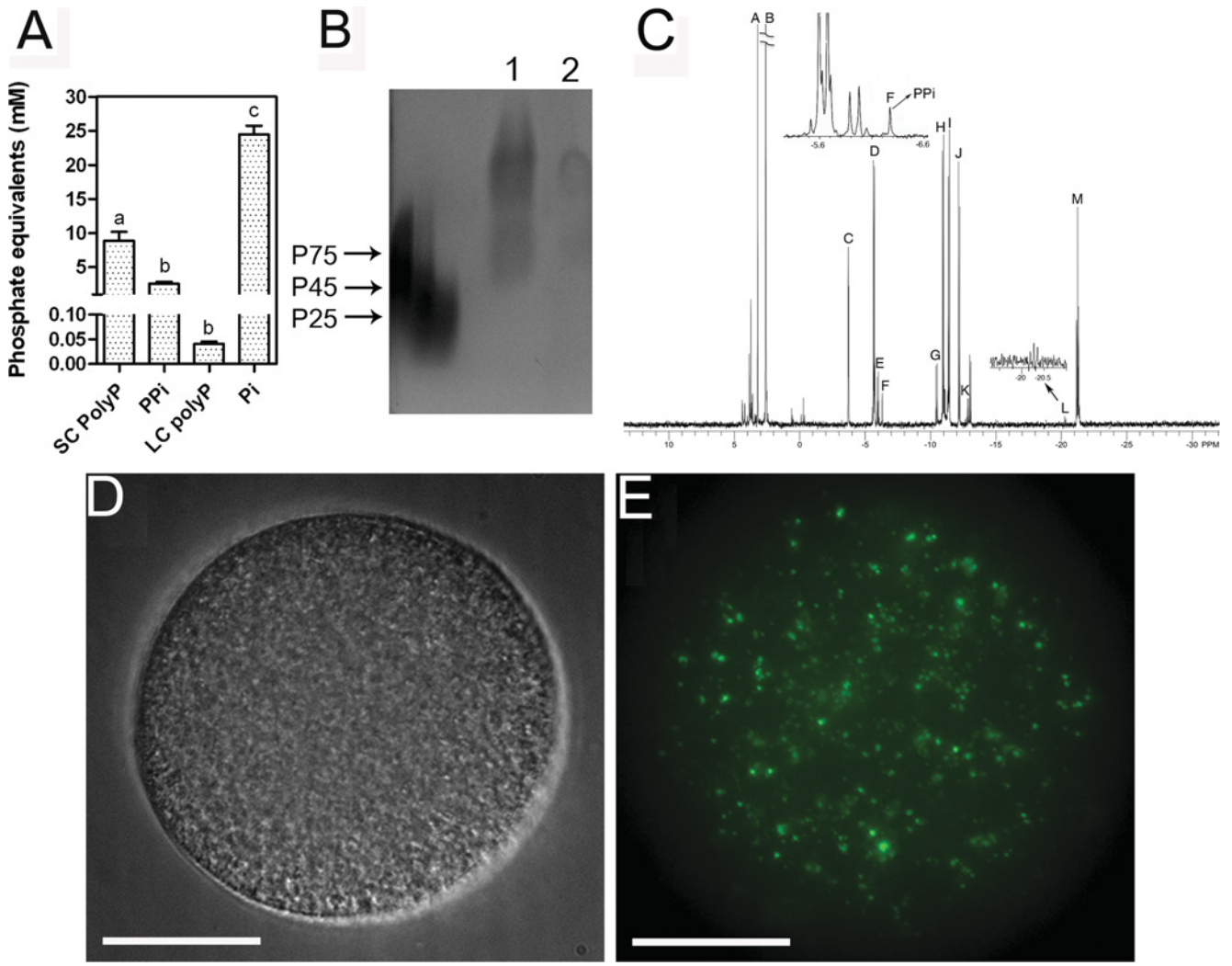


**Figure 3 Detection of $PP_i$ and poly P in sea urchin eggs**

(**A**) $PP_i$, SC poly P and LC poly P were assayed as described in the Materials and methods section, and levels are expressed as mM poly P (in terms of $P_i$ residues). Data are from four experiments, and show means ± S.E.M. Different letters indicate significant differences (one-way ANOVA, $P < 0.05$). (**B**) Agarose gel electrophoresis of poly P stained with Toluidine Blue. Lane 1, poly P extract; lane 2, poly P extract after rPPX1 treatment. P75, P45 and P24 are poly P standards of 75+, 45 and 25 phosphate units. (**C**) 242.8-MHz ($^1$H decoupled) $^{31}$P-NMR spectra of a perchloric acid extract of sea urchins eggs. See assignments in Table 1. (**D**) Differential interferential microscopy of the sea urchin egg shown in (**E**). (**E**) Localization of poly P using the recombinant PPBD of *E. coli* PPX linked with an Xpress epitope tag. Images were deconvolved for 15 cycles using Softwarx deconvolution software. Other conditions are described in the Materials and methods. Scale bars in (**D**) and (**E**) are 15 $\mu$m.

(Figure 2C). X-ray microanalysis of the less electron-dense granules, probably corresponding to yolk platelets (Figure 2B, white arrow), revealed only the presence of sulfur (Figure 2D), suggesting that they are rich in proteins. Copper arose from the Formvar-coated grids in both cases and was also detected in spectra taken from the background (results not shown).

### $PP_i$ and poly P in sea urchin eggs

One of the characteristics of acidocalcisomes is that they contain large amounts of SC and LC poly P, and also $PP_i$ [26]. As shown in Figure 3(A) egg homogenates contain ~220-fold more SC than LC poly P, whereas $PP_i$ content was approximately half the amount of SC poly P (all expressed in terms of $P_i$ residues for comparative purposes). Poly P was also detected by electrophoresis of extracts in 1 % agarose gels stained with Toluidine Blue (Figure 3B, lane 1), and pre-treatment of these samples with rPPX1 resulted in considerable decrease in staining (Figure 3B, lane 2).

Figure 3(C) shows a representative 242.8 MHz ($^1$H-decoupled) $^{31}$P-NMR spectrum of perchloric acid extracts of sea urchin eggs. Resonance assignments for this spectrum are given in Table 1. The predominant peak in the spectrum is $P_i$ (peak B). The inset region at ~ −6 p.p.m. (left-hand inset) contains the $PP_i$ resonance, peak F. The region between −19 and −22 p.p.m. is shown in the right-hand inset and contains peaks for the $\beta$-phosphate of nucleoside triphosphates (M), in addition to the central phosphate of poly P (L). The spectrum shows considerable amounts of phosphorylcholine (A) and phosphoarginine (C).

Poly P, as detected using the PPBD of *S. cerevisiae* PPX [37], was localized in small vesicles randomly distributed in the egg (Figures 3D and 3E, and Supplementary Movie S1). There was no poly P signal in the negative controls (i.e. in the absence of PPBD).

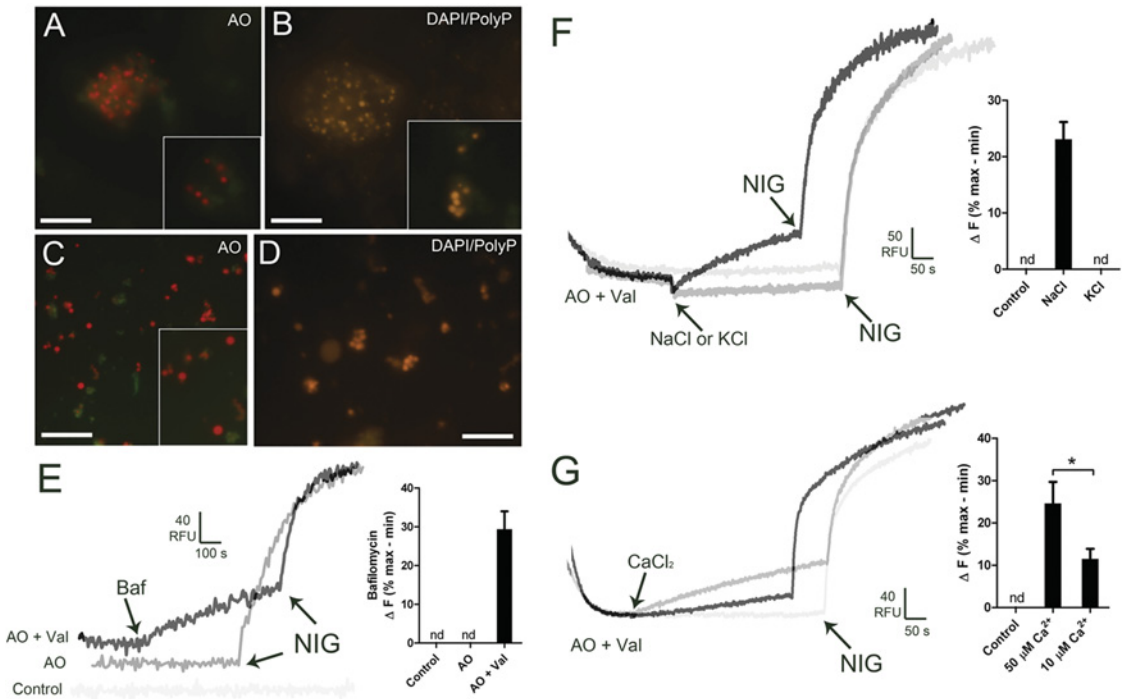


**Figure 4 Fluorescence microscopy and Acridine Orange release from dense granule fractions**

Dense granule fractions were incubated with 3 $\mu$M Acridine Orange [AO (**A** and **C**)] or 10 $\mu$g/ml DAPI (**B** and **D**) as described in the Materials and methods section. Note the accumulation of Acridine Orange [(**A** and **C**), orange] and DAPI [(**B** and **C**), yellow] in vesicles distributed in groups (**A** and **B**) or isolated (**C** and **D**). Scale bars in (**A**–**D**) are 5 $\mu$m. (**E**) The dense granule fraction was diluted in GluIM buffer in the presence of 6 $\mu$M Acridine Orange with and without 10 $\mu$M valinomycin (Val), and changes in fluorescence were monitored in a fluorimeter. Bafilomycin $A_1$ (Baf, 1 $\mu$M) and nigericin (NIG, 1 $\mu$M) were added where indicated. Grey trace (AO) is the control in the absence of valinomycin. Light grey trace (Control) is the control in the absence of additions. Tracings are representative of five experiments. The histogram summarizes the changes in fluorescence ($\Delta F$) in (**E**), and is shown as the means $\pm$ S.D of five determinations expressed as a percentage of the maximal nigericin response. (**F** and **G**) The dense granule fraction was pre-incubated with 3 $\mu$M Acridine Orange and 10 $\mu$M valinomycin until it equilibrated. (**F**) NaCl (100 mM; black trace) or 100 mM KCl (dark grey trace) and 5 $\mu$M nigericin were added where indicated. (**G**) $CaCl_2$ at 10 $\mu$M (black trace) or 50 $\mu$M (dark grey trace) and 5 $\mu$M nigericin were added where indicated. Control tracings without NaCl or KCl (**F**) or without $CaCl_2$ (**G**) are shown in light grey. Traces in (**F**) and (**G**) are representative of at least three experiments The histograms summarize the changes in fluorescence ($\Delta F$) in (**F**) and (**G**), and are shown as the means $\pm$ S.D of three determinations expressed as a percentage of the maximal nigericin response. Asterisks indicate significant differences (measured using a Student's *t* test, $P < 0.05$). Ordinates are scaled as RFU (relative fluorescence units) for (**E**–**G**).

**Table 1 $^{31}$P-NMR resonance assignments for perchloric acid extracts of sea urchin eggs**

*NTP, nucleoside triphosphate; #NDP, nucleoside diphosphate.

| Peak | Assignment | Chemical shift |
|---|---|---|
| A | Phosphorylcholine | 3.22 |
| B | $P_i$ | 2.60 |
| C | Phosphoarginine | −3.71 |
| D | $\gamma$-P of NTP* | −5.66 |
| E | $\beta$-P of NDP# | −5.97 |
| F | Inorganic $PP_i$ | −6.29 |
| G | $\alpha$-P of NDP# | −10.45 |
| H | $\alpha$-P of NTP* | −10.94 |
| I, J | NAD(H) | −11.39, −12.17 |
| K | NDP-glucose | −12.84 |
| L | Central P of LC poly P | −20.28 |
| M | $\beta$-P of NTP* | −21.21 |

## Isolation of dense granules and demonstration of their acidity and poly P content

To isolate the dense granules (Figure 2) and investigate their chemical and enzymatic content, we used iodixanol centrifugation as described in the Materials and methods section. The pellet fraction was applied to Formvar-coated grids, and direct observation showed the presence of multiple electron-dense granules of variable size (Supplementary Figure S1A at http://www.BiochemJ.org/bj/429/bj4290485add.htm). X-ray microanalysis (Supplementary Figures S1B and S1C) showed that most of these granules (15 out of 25) contained a similar elemental composition to that of dense granules in whole eggs or homogenates (Figure 2C). Standard transmission electron microscopy of this fraction revealed the presence of clear granules (corresponding to dense granules), which most of the time appeared empty or containing a residual electron-dense material, as previously observed in whole eggs (Figure 1), and some mitochondrial contamination (results not shown).

The presence of granules in the dense fraction was confirmed by incubation of the preparation in the presence of Acridine Orange. The Acridine Orange-stained granules appeared in groups (Figure 4A) or as isolated vesicles (Figure 4C). We also investigated the location of poly P using DAPI (Figures 4B and 4D). DAPI is known to shift its emission fluorescence to a maximum wavelength of 525 nm (yellow) in the presence of poly P, this change being specific for poly P and not produced by $PP_i$ or other anions [31]. We detected the staining of numerous vesicles, either in groups (Figure 4B) or isolated (Figure 4D). No staining was detected when DAPI was omitted (results not shown).

Work by Morgan and Galione [6] has shown that acidification of granules in sea urchin eggs is maintained by a V-$H^+$-ATPase

(vacuolar type $H^+$-ATPase), as happens with other acidic organelles, including the acidocalcisomes of *Trypanosoma cruzi* [39], *Trypanosoma brucei* [40], *D. discoideum* [28], *C. reinhardtii* [27] and human platelets [31]. Interestingly, the function of this proton pump could be demonstrated only by inhibition of acidification by bafilomycin $A_1$ after pre-incubation of the preparation with either valinomycin or FCCP (carbonyl cyanide *p*-trifluoromethoxyphenylhydrazone) [6]. In agreement with those results, bafilomycin $A_1$ released Acridine Orange after pre-incubation of the dense granule fractions with valinomycin (Figure 4E, black trace), but not in its absence (Figure 4E, grey trace), although this could be accomplished by nigericin (Figure 4E, grey trace). Addition of nigericin after bafilomycin $A_1$ completed the release of Acridine Orange from the vesicles (Figure 4E, black trace).

### Evidence for $Na^+/H^+$ and $Ca^{2+}/H^+$ exchange activities in dense granules

Acidocalcisomes of *T. brucei* [40,41] and *Leishmania donovani* [42,43] have been reported to contain $Na^+/H^+$ and $Ca^{2+}/H^+$ exchangers and the coupled interaction of these exchangers was postulated to result in a mechanism of $Ca^{2+}$ release upon alkalinization or $Na^+$ entry into acidocalcisomes [42]. Experiments on enriched dense granule fractions showed the presence of these ion-exchange mechanisms. For example, addition of 100 mM NaCl (Figure 4F, black trace), but not of 100 mM KCl (Figure 4F, light grey trace) resulted in Acridine Orange efflux, suggesting the activity of a $Na^+/H^+$ exchanger in the dense granule fraction. Addition of 10 and 50 $\mu$M $CaCl_2$ under similar conditions also resulted in Acridine Orange efflux (Figure 4G, black and dark grey traces respectively), suggesting the operation of a $Ca^{2+}/H^+$ exchanger, and the potential function of these exchangers as a mechanism of $Ca^{2+}$ release upon alkalinization of dense granules [43]. Under physiological conditions, these exchangers could contribute to $Na^+$ and $Ca^{2+}$ uptake into these acidic compartments, as occurs with the plant vacuole [44].

### Association of $Ca^{2+}$ release and poly P hydrolysis

It has been shown that $Ca^{2+}$ release from acidocalcisomes of *T. cruzi* occurs in parallel with poly P hydrolysis [34]. We therefore investigated whether there was a correlation between $Ca^{2+}$ release from the acidic compartment containing poly P in the sea urchin egg dense granule fraction and poly P hydrolysis. Addition of nigericin resulted in $Ca^{2+}$ release from the dense granule fraction, as detected by changes in the fluorescence of Fluo-3 (Figure 5A) and this resulted in a significant decrease in the levels of SC poly P, but not in the levels of LC poly P (Figure 5C). Addition of nigericin also resulted in alkalinization of the vesicles (Figure 5B) confirming the link between alkalinization of acidocalcisomes and $Ca^{2+}$ release.

### Degradation of poly P and $PP_i$ in dense granules

Acidocalcisomes are known to possess enzymes linked to $PP_i$ and poly P metabolism [26]. The rapid hydrolysis of poly P that occurs when $Ca^{2+}$ release is stimulated by nigericin (Figure 5) suggested the presence of an PPX activity in the dense granule fraction. To know whether this was the case, we investigated $PP_i$ and poly P hydrolysis by dense granule fractions. Hydrolysis of poly $P_3$ (Figure 6A) or $PP_i$ (Figure 6B) was approximately linear with time, whereas hydrolysis of poly $P_{75+}$ stopped after 5 min. This probably indicates the hydrolysis of contaminating SC poly Ps in

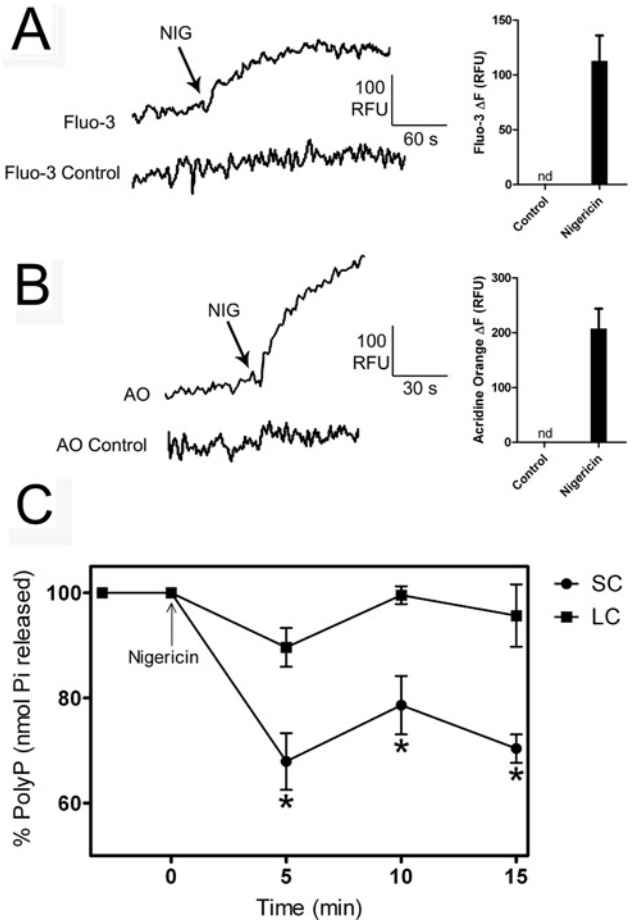


**Figure 5 Effects of nigericin on calcium release, acidity and poly P content of dense granule fractions**

(**A**) The dense granule fraction was incubated in GluIM in the presence of Fluo-3, and nigericin (5 $\mu$M) was added at the time indicated. (**B**) The dense granule fraction was pre-incubated with 3 $\mu$M Acridine Orange until it equilibrated, and nigericin (5 $\mu$M) was added at the time indicated. (**C**) SC and LC poly P levels were measured at different times after the addition of 10 $\mu$M nigericin. Tracings in (**A**) and (**B**) are representative of at least four experiments. Ordinates are scaled as RFU (relative fluorescence units). Controls without nigericin addition (**A** and **B**) are shown. The graph in (**C**) shows means $\pm$ S.E.M. for three experiments. Asterisks in (**C**) indicate significant differences (one-way ANOVA, $P < 0.05$).

the poly $P_{75+}$ sample (which is a mixture of poly P molecules with a mean length of 84), and the inability of the polyphosphatase to cleave LC poly Ps.

### NAADP-stimulated $Ca^{2+}$ release from dense granules is not accompanied by hydrolysis of poly P and the fraction is not sensitive to GPN

NAADP has been shown to release $Ca^{2+}$ from acidic granules of sea urchin eggs [4], whereas $IP_3$ releases $Ca^{2+}$ from the ER [2]. Figures 7(A) and 7(D) show that both NAADP and $IP_3$ were able to release comparable amounts of $Ca^{2+}$ from vesicular compartments in egg homogenates. A second addition of NAADP showed no response revealing desensitization (results not shown). NAADP (Figure 7B) or $IP_3$ (Figure 7E) were, however, less efficacious in the dense granule fraction. We next tested whether poly P hydrolysis occurred as a consequence of $Ca^{2+}$ release by NAADP in dense granule fractions, but no significant changes were detected (Figure 7G). The lack of enrichment in NAADP-sensitive calcium stores, together with the lack of poly

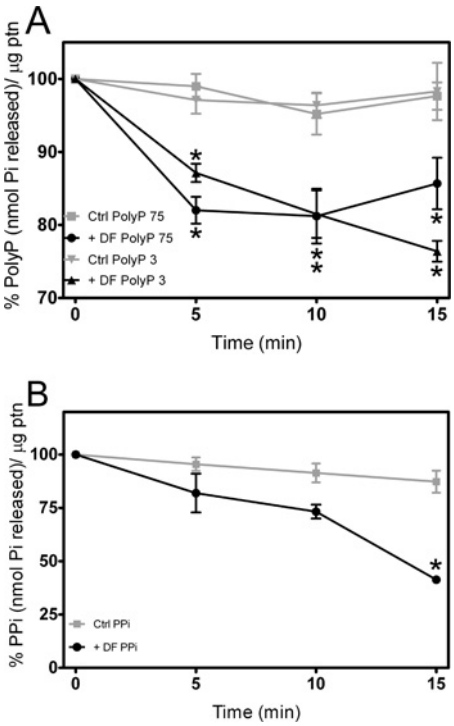


**Figure 6 Poly P and $PP_i$ hydrolysis in dense granule fractions**

Dense granule fractions (DF) were homogenized in GluIM buffer and tested for PPX and PPase activities as described in the Materials and methods section. (**A**) Levels of poly $P_3$ and poly $P_{75+}$ after different times of incubation with the dense granule fraction. (**B**) Levels of $PP_i$ after different times of incubation with the dense granule fraction. Controls (Ctrl) are the substrates incubated in buffer, with no fraction added. Graphs show mean relative activities ± S.E.M. for four experiments. Asterisks indicate significant differences (one-way ANOVA, $P < 0.05$).

P hydrolysis accompanying calcium release by NAADP suggests that the acidocalcisome-related organelles of sea urchin eggs are not the calcium stores sensitive to NAADP.

The presence of releasable $Ca^{2+}$ in lysosomes has been demonstrated based on experiments using GPN and it has been reported that NAADP-targeted stores are sensitive to GPN [4]. GPN is a lysosome-disrupting cathepsin-C substrate that was originally used to distinguish lysosomes, which contain cathepsin C, from pre-lysosomal endocytic vacuoles, which do not [25]. Hydrolysis of GPN by cathepsin C induces osmotic swelling of the lysosome and release of its content, including $Ca^{2+}$, into the cytoplasm. Treatment of sea urchin homogenates with GPN caused $Ca^{2+}$ release, which was completed by nigericin (Figure 7H, trace TH). In contrast, addition of GPN to dense granule fractions did not cause $Ca^{2+}$ release (Figure 7H, trace DF) suggesting that this fraction is not contaminated with lysosomes.

### Use of stratified eggs reveals that dense granules localize to the centripetal pole of the egg

As discussed above, when eggs are stratified by centrifugation, yolk platelets localize to the centrifugal pole which is the site where higher $Ca^{2+}$ release occurs upon local photolysis of caged NAADP and which is opposite to the nucleus and lipid droplets, where clear granules localize [24]. When eggs were stratified and stained with either PPBD (Supplementary Figures S2B and S2C at http://www.BiochemJ.org/bj/429/bj4290485add.htm) or DAPI (Supplementary Figures S2E and S2F), staining was detected in the centripetal pole in agreement with the reported localization of the clear granules [24] and with the results showing negligible NAADP-stimulated $Ca^{2+}$ release by dense granule fractions. In contrast, staining with LysoTracker Red was in the centrifugal pole, where the yolk platelets localize and where higher NAADP-stimulated $Ca^{2+}$ release has been detected [4] (Supplementary Figures S2G–S2J).

## DISCUSSION

We report in the present paper that sea urchin eggs are rich in poly P. Poly P was detected by a biochemical method based on its specific hydrolysis by a PPX, by Toluidine Blue staining in agarose gels, by $^{31}$P-NMR and by a recently developed method based on staining with the specific poly-P-binding region of *S. cerevisiae* PPX [37]. This was confirmed by visualization of poly P in the dense granule fraction using DAPI and by its hydrolysis when nigericin released $Ca^{2+}$ from these fractions. We also found considerable amounts of phosphoarginine, a phosphagen present in many invertebrates although not previously reported in sea urchin eggs [45].

Our results also suggest that the dense granules of sea urchin eggs, which could correspond to the clear granules detected by transmission electron microscopy (both large and small; Figure 1) have many characteristics in common with acidocalcisomes [26]: (i) they are acidic due to the operation of a bafilomycin $A_1$-sensitive vacuolar ATPase and are able to accumulate acidophilic dyes such as Acridine Orange; (ii) they can store extremely large amounts of calcium and other cations such as magnesium, sodium and zinc, and can release $Ca^{2+}$ in the presence of nigericin; (iii) they contain very large amounts of phosphorus in the form of phosphate, $PP_i$, and poly P; (iv) they have very high electron density, when examined by energy-filtering transmission electron microscopy, and have an empty appearance with condensed material in their interior, when examined by standard transmission electron microscopy; and (v) they possess activities commonly found in acidocalcisomes, such as PPase [46], PPX [47], and $Ca^{2+}/H^+$ and $Na^+/H^+$ exchangers [40–43].

Clear granules are distributed at random in unfertilized sea urchin eggs [21], in agreement with the distribution of poly P-labelled granules (Figure 3E, and Supplementary Movie S1). The function of these clear granules is unknown, but their composition, investigated in the present study, implies an important role in storage of phosphorus and cations needed for embryo development. Our results suggest that, although these granules are acidic and contain large amounts of calcium, they are not the targets for NAADP-stimulated $Ca^{2+}$ release.

It has been reported that fertilization induces pH changes in acidic stores of sea urchin eggs [5], and we have demonstrated that alkalinization of dense granules leads to $Ca^{2+}$ release and poly P hydrolysis. Alkalinization of acidic stores of the sea urchin egg could be either upon vesicle fusion with the plasma membrane, when the alkaline extracellular medium exchanges with the acidic lumen of cortical granules that are the primary egg exocytic vesicles, or upon $Ca^{2+}$ release from yolk platelets stimulated by NAADP [5]. It has been reported that cortical alkalinization coincides with NAADP-induced $Ca^{2+}$ release from intracellular stores [5], and that this alkalinization appears to occur at the individual vesicle level [5]. Alkalinization of yolk platelets is increased by NAADP by a mechanism coupled to $Ca^{2+}$ release via the NAADP receptor [5]. It has been proposed that the fall in the luminal [$Ca^{2+}$] allows $H^+$ to bind to vacated sites on a luminal polyanionic matrix, thus resulting in alkalinization of the store [6].

In addition to acidic store alkalinization, it has been shown that fertilization of sea urchin eggs led to a change in cytosolic pH

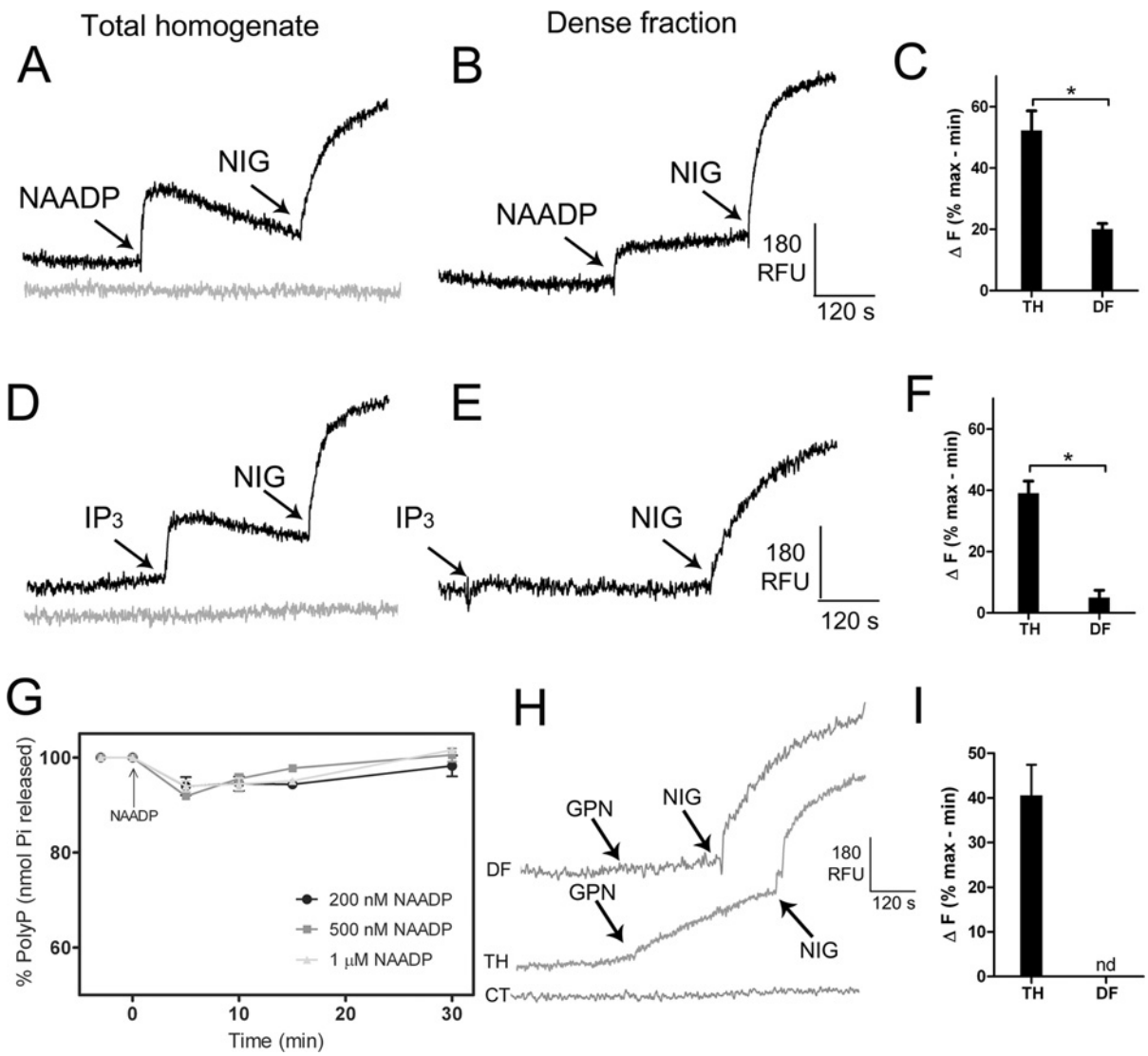


**Figure 7 Effect of $Ca^{2+}$-releasing agents on poly P content of dense granule fractions**

Total homogenates (**A** and **D**) and dense granule fractions (**B** and **E**) (310 $\mu$g of protein in each case) were tested for calcium release triggered by $IP_3$ and NAADP. Preparations were incubated in GluIM buffer in the presence of 3 $\mu$M Fluo-3 as described in the Materials and methods section. $IP_3$ (300 nM), NAADP (200 nM) and nigericin (5 $\mu$M) were added where indicated. Tracings are representative of at least four experiments. Controls without additions are shown in grey. Ordinates are scaled as RFU (relative fluorescence units). (**C** and **F**) The histograms summarize the changes in fluorescence ($\Delta F$) in (**A** and **B**) and (**D** and **E**) respectively, and are shown as the means $\pm$ S.D. for three experiments expressed as a percentage of the maximal nigericin response. Asterisks indicate significant differences (measured using a Student's *t* test, $P < 0.05$). (**G**) SC poly P levels were measured at different times after the addition of increasing NAADP concentrations. Graph shows means $\pm$ S.E.M. for three experiments. (**H**) Dense granule fractions (trace 1) and total homogenate (trace 2) were incubated in GluIM in the presence of 3 $\mu$M Fluo-3. GPN (100 $\mu$M) and nigericin (5 $\mu$M) were added at the times indicated. The control with no additions is shown in trace 3. Ordinates are scaled as RFU (relative fluorescence units). (**I**) The histogram summarizes the changes in fluorescence ($\Delta F$) in (**H**), and shows the means $\pm$ S.D of four determinations expressed as a percentage of the maximal nigericin response.

from 6.9 to 7.3 with a concomitant acidification of the sea water, and that the egg remains alkaline for approx. 60 min [48,49]. This change in cytosolic pH is driven by a plasma membrane $Na^+/H^+$ exchanger [48]. An increase in cytosolic sodium has been shown previously to increase the release of calcium from acidocalcisomes of *T. brucei* [40,41] and *L. donovani* [42,43], and this could potentially occur with the sea urchin egg dense granules. It has also been shown that suspension of sea urchin eggs in $NH_4Cl$ (5 mM, pH 8.0), which could lead to alkalinization of all acidic granules, stimulates their metabolism and ability to undergo chromosome replication and condensation without triggering the cortical granule reaction [50]. Therefore we cannot rule out that alkalinization of dense granules could lead to an additional $Ca^{2+}$ release.

Previous studies have indicated that the acidic compartments responsible for $Ca^{2+}$ release induced by NAADP are lysosome-like organelles [4], possibly the yolk platelets [5]. This was based on experiments showing that GPN-mediated disruption of the organelles reduced the response to photoreleased or microinjected free NAADP, and on the response of yolk-platelet-enriched fractions to NAADP [4]. The lack of calcium detection in yolk platelets in our X-ray microanalyses (Figure 2D) does not indicate its absence, but simply that the amount of calcium present is below the limit of detection of this technique, which cannot discriminate between bound and free calcium. Yolk platelets would then be equivalent to the lysosomes of mammalian cells that are emerging as important calcium stores [51], whereas the clear (dense) granules would be,

as acidocalcisomes, equivalent to lysosome-related organelles [51].

NAADP-induced $Ca^{2+}$ signals are small and possibly localized, but can trigger ER $Ca^{2+}$ mobilization through $Ca^{2+}$-induced $Ca^{2+}$ release via $IP_3$ and ryanodine receptors [17], thus explaining the extensive $Ca^{2+}$ waves detected after fertilization. Alkalinization of the cytosol and $Ca^{2+}$ release from dense granules (acidocalcisomes) could also contribute to these $Ca^{2+}$ waves. Supplementary Figure S3 (at http://www.BiochemJ.org/bj/429/bj4290485add.htm) shows a model of the $Ca^{2+}$ mobilization pathways that could be involved in sea urchin eggs. NAADP would trigger $Ca^{2+}$ release from yolk platelets that could then trigger ER $Ca^{2+}$ mobilization through $Ca^{2+}$-induced $Ca^{2+}$ release via $IP_3$ and ryanodine receptors. Alkalinization of the egg cytoplasm by $Na^+$ entry would release additional $Ca^{2+}$ from dense granules (acidocalcisomes). Therefore acidocalcisomes, which are randomly distributed, could contribute to the NAADP-mediated two-phase $Ca^{2+}$ release response. Alkalinization of these acidocalcisomes would lead to the hydrolysis of poly P, which would provide an important source of $P_i$ for the anabolic reactions necessary for embryogenesis.

## AUTHOR CONTRIBUTION

Isabela Ramos performed most of the experiments and participated in planning and writing of the paper; Douglas Pace assisted in sea urchin egg preparation and writing of the paper; Katherine Verbist prepared the recombinant PPBD of *E. coli* PPX; Fu-Yang Lin, Yonghui Zhang and Eric Oldfield carried out the NMR experiments and interpreted the results; Kildare Miranda, Ednildo Machado and Wanderley de Souza assisted in the design of the study, planning and manuscript preparation; and Roberto Docampo designed the study, and participated in planning and writing of the paper.

## ACKNOWLEDGEMENTS

We thank the late Professor Arthur Kornberg for *E. coli* CA38 pTrcPPX1, and Dr Katsuharu Saito for *E. coli* DH5a pTrc-PPBD.

## FUNDING

This work was supported by the Georgia Research Alliance/Barbara and Sanford Orkin Chair in Tropical and Emerging Global Diseases and Cellular Biology (to R.D.); I.B.R. was supported, in part, by a training grant from the Ellison Medical Foundation to the Center for Tropical and Emerging Global Diseases. D.A.P. was partially supported by the National Institutes of Health [NIH T32 training grant number AI-060546]. E.O., F.-Y.L and Y.Z. were supported, in part, by the National Institutes of Health [grant number GM-065307]. I.B.R., K.M., E.A.M. and W.S. were supported, in part, by the Fundação de Amparo a Pesquisa do Estado de Rio de Janeiro (FAPERJ) and the Conselho Nacional de Desenvolvimento Científico e Tecnológico (CNPq, Brazil).

## REFERENCES

1 Parrington, J., Davis, L. C., Galione, A. and Wessel, G. (2007) Flipping the switch: how a sperm activates the egg at fertilization. Dev. Dyn. **236**, 2027–2038
2 Clapper, D. L., Walseth, T. F., Dargiem, P. J and Lee, H.C. (1987) Pyridine nucleotide metabolites stimulate calcium release from sea urchin egg microsomes desensitized to inositol trisphosphate. J. Biol. Chem. **262**, 9561–9568
3 Lee, H. C. and R., Aarhus (1995) A derivative of NADP mobilizes calcium stores insensitive to inositol trisphosphate and cyclic ADP-ribose. J. Biol. Chem. **270**, 2152–2157
4 Churchill, G. C., Okada, Y., Thomas, J. M., Genazzani, A. A., Patel, S. and Galione, A. (2002) NAADP mobilizes $Ca^{2+}$ from reserve granules, lysosome-related organelles, in sea urchin eggs. Cell **111**, 703–708
5 Morgan, A. J. and Galione, A. (2007) Fertilization and nicotinic acid adenine dinucleotide phosphate induce pH changes in acidic $Ca^{2+}$ stores in sea urchin eggs. J. Biol. Chem. **282**, 37730–37737
6 Morgan, A. J. and Galione, A. (2007) NAADP induces pH changes in the lumen of acidic $Ca^{2+}$ stores. Biochem. J. **402**, 301–310
7 Yamasaki, M., Thomas, J. M., Churchill, G. C., Garnham, C., Lewis, A. M., Cancela, J. M., Patel, S. and Galione, A. (2005) Role of NAADP and cADPR in the induction and maintenance of agonist-evoked $Ca^{2+}$ spiking in mouse pancreatic acinar cells. Curr. Biol. **15**, 874–878
8 Mitchell, K . J., Lai, F. A. and Rutter, G. A. (2003) Ryanodine receptor type I and nicotinic acid adenine dinucleotide phosphate receptors mediate $Ca^{2+}$ release from insulin-containing vesicles in living pancreatic beta-cells (MIN6). J. Biol. Chem. **278**, 11057–11064
9 Zhang, F., Zhang, G., Zhang, A. Y., Koeberl, M. J., Wallander, E. and Li, P. L. (2006) Production of NAADP and its role in $Ca^{2+}$ mobilization associated with lysosomes in coronary arterial myocytes. Am. J. Physiol. Heart Circ. Physiol. **291**, H274—H282
10 Brailoiu, E., Hoard, J. L., Filipeanu, C. M., Brailoiu, G. C., Dun, S L., Patel, S. and Dun, N. J. (2005) Nicotinic acid adenine dinucleotide phosphate potentiates neurite outgrowth. J. Biol. Chem. **280**, 5646–56450
11 Mándi, M., Tóth, B., Timár, G. and Bak, J. (2006) $Ca^{2+}$ release triggered by NAADP in hepatocyte microsomes. Biochem. J. **395**, 233–238
12 Steen, M., Kirchberger, T. and Guse, A. H. (2007) NAADP mobilizes calcium from the endoplasmic reticular $Ca^{2+}$ store in T-lymphocytes. J. Biol. Chem. **282**, 18864–18871
13 Zhang, F. and Li, P. L. (2007) Reconstitution and characterization of a nicotinic acid adenine dinucleotide phosphate (NAADP)-sensitive $Ca^{2+}$ release channel from liver lysosomes of rats. J. Biol. Chem. **282**, 25259–25269
14 Cancela, J. M., Churchill, G. C. and Galione, A. (1999) Coordination of agonist-induced $Ca^{2+}$-signalling patterns by NAADP in pancreatic acinar cells. Nature **398**, 74–76
15 Churchill, G. C. and Galione, A. (2001) NAADP induces $Ca^{2+}$ oscillations via a two-pool mechanism by priming $IP_3$- and cADPR-sensitive $Ca^{2+}$ stores. EMBO J. **20**, 2666–2671
16 Calcraft, P. J., Ruas, M, Pan, Z., Cheng, X., Arredouani, A., Hao, X., Tang, J., Rietdorf, K., Teboul, L., Chuang, K. T. et al. (2009) NAADP mobilizes calcium from acidic organelles through two-pore channels. Nature **459**, 596–600
17 Brailoiu, E., Churamani, D., Cai, X., Schrlau, M. G., Brailoiu, G. C., Gao, X., Hooper, R., Boulware, M. J., Dun, N. J., Marchant, J. S. and Patel, S. (2009) Essential requirement for two-pore channel 1 in NAADP-mediated calcium signaling. J. Cell Biol. **186**, 201–209
18 Zong, X., Schieder, M., Cuny, H., Fenske, S., Gruner, C., Rötzer, K., Griesbeck, O., Harz, H., Biel, M. and Wahl-Schott, C. (2009) The two-pore channel TPCN2 mediates NAADP-dependent $Ca^{2+}$-release from lysosomal stores. Pflugers Arch. **458**, 891–899
19 Brailoiu, E., Hooper, R., Cai, X., Brialoiu, G. C., Keebler, M. V., Dun, N. J., Marchant, J. S. and Patel, S. (2010) J. Biol. Chem. **285**, 2897–2901
20 Terasaki, M. and Jaffe, L. A. (2004) Labeling of cell membranes and compartments for live cell fluorescence microscopy. Methods Cell Biol. **74**, 469–489
21 Lee, H. C. and Epel, D. (1983) Changes in intracellular acidic compartments in sea urchin eggs after activation. Dev. Biol. **98**, 446–454
22 Sardet, C. (1983) The ultrastructure of the sea urchin egg cortex isolated before and after fertilization. Dev. Biol. **105**, 196–210
23 Mallya, S. K., Partin, J. S., Valdizan, M. C. and Lennarz, W. J. (1992) Proteolysis of the major yolk glycoproteins is regulated by acidification of the yolk platelets in sea urchin embryos. J. Cell Biol. **117**, 1211–1221
24 Lee, H. C. and Aarhus, R. (2000) Functional visualization of the separate but interacting calcium stores sensitive to NAADP and cyclic ADP-ribose. J. Cell Sci. **113**, 4413–4420
25 Jadot, M., Colmant, C., Wattiaux-De Coninck, S. and Wattiaux, R. (1984) Intralysosomal hydrolysis of glycyl-L-phenylalanine 2-naphthylamide. Biochem. J. **219**, 965–970
26 Docampo, R., de Souza, W., Miranda, K., Rohloff, P. and Moreno, S. N. J. (2005) Acidocalcisomes: conserved from bacteria to man. Nat. Rev. Microbiol. **3**, 251–261
27 Ruiz, F. A., Marchesini, N., Seufferheld, M. and Govindjee, Docampo, R. (2001) The polyphosphate bodies of *Chlamydomonas reinhardtii* possess a proton-pumping pyrophosphatase and are similar to acidocalcisomes. J. Biol. Chem. **276**, 46196–46203
28 Marchesini, N., Ruiz, F. A., Vieira, M. and Docampo, R. (2002) Acidocalcisomes are functionally linked to the contractile vacuole of *Dictyostelium discoideum*. J. Biol. Chem. **277**, 8146–8153
29 Seufferheld, M., Vieira, M., Ruiz, F. A., Rodrigues, C. O., Moreno, S. N. J. and Docampo, R. (2003) Identification of organelles in bacteria similar to acidocalcisomes of unicellular eukaryotes. J. Biol. Chem. **278**, 29971–29978
30 Seufferheld, M., Lea, C. R., Vieira, M., Oldfield, E. and Docampo, R. (2004) The $H^+$-pyrophosphatase of *Rhodospirillum rubrum* is predominantly located in polyphosphate-rich acidocalcisomes. J. Biol. Chem. **279**, 51193–51202
31 Ruiz, F. A., Lea, C. R., Oldfield, E. and Docampo, R. (2004) Human platelet dense granules contain polyphosphate and are similar to acidocalcisomes of bacteria and unicellular eukaryotes. J. Biol. Chem. **279**, 44250–44257
32 Motta L.S., Ramos I. B., Gomes F.M., de Souza W., Champagne D.E., Santiago M. F., Docampo, R., Miranda, K. and Machado, E.A. (2009) Proton-pyrophosphatase and polyphosphate in acidocalcisome-like vesicles from oocytes and eggs of *Periplaneta americana*. Insect Biochem. Mol. Biol. **39**, 198–206

33 Ramos, I. B., Miranda, K., Ulrich, P, Ingram, P, LeFurgey, A., Machado, E. A., de Souza, W. and Docampo, R. (2010) Calcium- and polyphosphate-containing acidocalcisomes in chicken egg yolk. Biol. Cell **102**, 421–434

34 Ruiz, F. A., Rodrigues, C. O. and Docampo, R. (2001) Rapid changes in polyphosphate content within acidocalcisomes in response to cell growth, differentiation, and environmental stress in *Trypanosoma cruzi*. J. Biol. Chem. **276**, 26114–26121

35 Ault-Riche, D., Fraley, C D., Tzeng, C M. and Kornberg, A. (1998) Novel assay reveals multiple pathways regulating stress-induced accumulations of inorganic polyphosphate in *Escherichia coli*. J. Bacteriol. **180**, 1841–1847

36 Lanzetta, P. A., Alvarez, L. J., Reinach, P. S. and Candia, O. A. (1979) An improved assay for nanomole amounts of inorganic phosphate. Anal. Biochem. **100**, 95–97

37 Saito, K., Ohtomo, R., Kuga-Uetake, Y., Aono, T. and Saito, M. (2005) Direct labeling of polyphosphate at the ultrastructural level in *Saccharomyces cerevisiae* by using the affinity of the polyphosphate binding domain of *Escherichia coli* exopolyphosphatase. Appl. Environ. Microbiol. **71**, 5692–5701

38 Afzelius, B. A. (1956) The ultrastructure of the cortical granules and their products in the sea urchin egg as studied with the electron microscope. Exp. Cell Res. **10**, 257–285

39 Lu, H. G., Zhong, L., de Souza, W., Benchimol, M., Moreno, S. N. J. and Docampo, R. (1998) $Ca^{2+}$ content and expression of an acidocalcisomal calcium pump are elevated in intracellular forms of *Trypanosoma cruzi*. Mol. Cell. Biol. **18**, 2309–2323

40 Rodrigues, C. O., Scott, D. A. and Docampo, R. (1999) Characterization of a vacuolar pyrophosphatase in *Trypanosoma brucei* and its localization to acidocalcisomes. Mol. Cell. Biol. **19**, 7712–7723

41 Vercesi, A. and Docampo, R. (1996) Sodium-proton exchange stimulates $Ca^{2+}$ release from acidocalcisomes of *Trypanosoma brucei*. Biochem. J. **315**, 265–270

42 Rodrigues, C. O., Scott, D. A. and Docampo, R. (1999) Presence of a vacuolar $H^+$-pyrophosphatase in promastigotes of *Leishmania donovani* and its localization to a different compartment from the vacuolar $H^+$-ATPase. Biochem. J. **340**, 759–766

43 Vercesi, A., Rodrigues, C. O., Catisti, R. and Docampo, R. (2000) Presence of a $Na^+/H^+$ exchanger in acidocalcisomes of *Leishmania donovani* and their alkalinization by anti-leishmanial drugs. FEBS Lett. **473**, 203–206

44 Maeshima, M. (2001) Tonoplast transporters: organization and function. Annu. Rev. Plant Physiol. Plant Mol. Biol. **52**, 469–497.

45 Ratto, A. and Christen, R. (1988) Purification and characterization of arginine kinase from sea-urchin eggs. Eur. J. Biochem. **173**, 667–674

46 Lemercier, G., Espiau, B., Ruiz, F. A., Vieira, M., Luo, S., Baltz, T., Docampo, R. and Bakalara, N. (2004) A pyrophosphatase regulating polyphosphate metabolism in acidocalcisomes is essential for *Trypanosoma brucei* virulence in mice. J. Biol. Chem. **279**, 3420–3425

47 Rodrigues, C. O., Ruiz, F. A., Vieira, M., Hill, J. E. and Docampo, R. (2002) An acidocalcisomal exopolyphosphatase from *Leishmania major* with high affinity for short chain polyphosphate. J. Biol. Chem. **277**, 50899–50906.

48 Johnson, J. D. and Epel, D. (1976) Intracellular pH and activation of sea urchin eggs after fertilisation. Nature **262**, 661–664

49 Shen, S. S. and Steinhardt, R. A. (1978) Direct measurement of intracellular pH during metabolic derepression of the sea urchin egg. Nature **272**, 253–254

50 Epel, D. and Carroll, Jr, E. J. (1975) Molecular mechanisms for prevention of polyspermy. Res. Reprod. **7**, 2–3

51 Patel, S. and Docampo, R. (2010) Acidic calcium stores open for business: expanding the potential for intracellular $Ca^{2+}$ signaling. Trends Cell Biol. **20**, 277–286


Received 23 December 2009/6 May 2010; accepted 24 May 2010
Published as BJ Immediate Publication 24 May 2010, doi:10.1042/BJ20091956

Biochem. J. (2010) **429**, 485–495 (Printed in Great Britain) doi:10.1042/BJ20091956

multimedia online data

## SUPPLEMENTARY ONLINE DATA

# Calcium- and polyphosphate-containing acidic granules of sea urchin eggs are similar to acidocalcisomes, but are not the targets for NAADP

Isabela B. RAMOS*†, Kildare MIRANDA†‡, Douglas A. PACE*, Katherine C. VERBIST*, Fu-Yang LIN§, Yonghui ZHANG‖, Eric OLDFIELD§‖, Ednildo A. MACHADO†‡, Wanderley DE SOUZA† and Roberto DOCAMPO*[1]

*Department of Cellular Biology and Center for Tropical and Emerging Global Diseases, University of Georgia, Athens, GA 30602, U.S.A., †Instituto de Biofísica Carlos Chagas Filho, and Instituto Nacional de Ciência e Tecnologia em Bioimagens e Biologia Estrutural, Universidade Federal do Rio de Janeiro, Rio de Janeiro, RJ 21941, Brazil, ‡Instituto Nacional de Metrologia Normalização e Qualidade Industrial, Diretoria de Programas, Xerém, Rio de Janeiro, RJ 25250, Brazil, §Center for Biophysics and Computational Biology, University of Illinois at Urbana-Champaign, Urbana, IL 61801, U.S.A., and ‖Department of Chemistry, University of Illinois at Urbana-Champaign, Urbana, IL 61801, U.S.A.

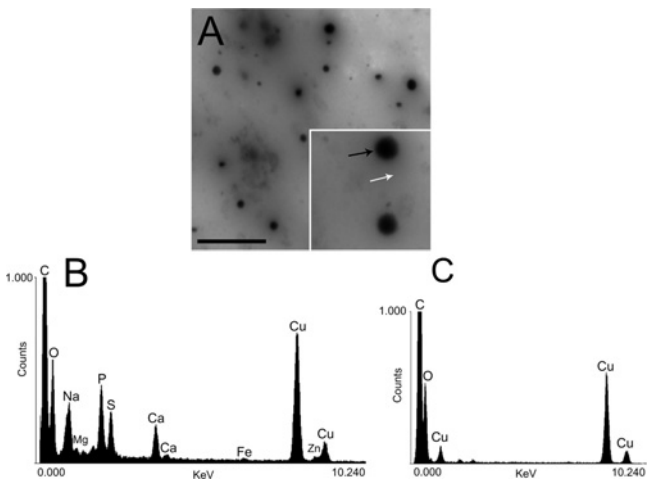


**Figure S1 Electron microscopy and X-ray microanalysis of the dense granule fraction**

(**A**) Direct observation of unfixed and unstained dense granules air-dried directly on to microscope grids. (**B**) Typical X-ray microanalysis spectrum of dense granules (black arrow). (**C**) Control spectrum of an adjacent area (white arrow). Scale bars in (**A**) are 0.5 $\mu$m.

[1] To whom correspondence should be addressed (email rdocampo@uga.edu).

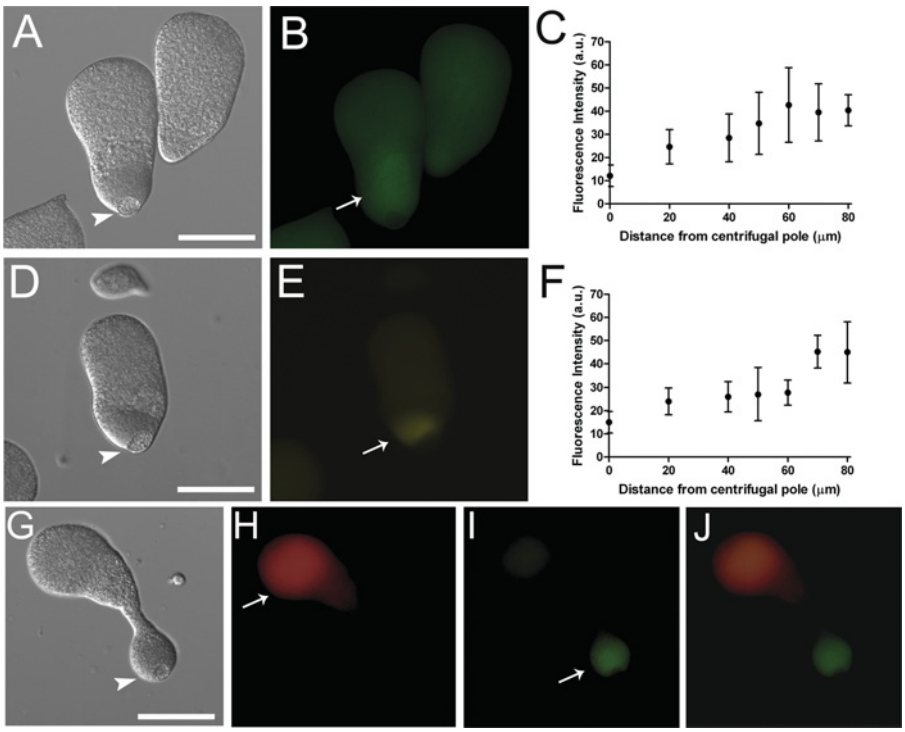


**Figure S2 Segregation of poly P stores in stratified sea urchin eggs**

(**A**, **B** and **C**) Sea urchin eggs were stratified and poly P stores were localized using the recombinant PPBD of *E. coli* PPX linked with an Xpress epitope tag. (**D, E** and **F**) Stratified eggs after DAPI incubation for poly P localization. (**C** and **F**) Fluorescence intensity profile plots of PPBD and DAPI staining respectively. Graphs show means ± S.D. for five eggs. (**G, H, I** and **J**) Sea urchin eggs were incubated with LysoTracker Red, stratified and then fixed and stained with PPBD as described in the Materials and methods section of the main text. (**G**) Differential interferential contrast microscopy image of one stratified egg. (**H, I** and **J**) LysoTracker, PPBD and merged corresponding images of (**G**) respectively. Arrows in (**B, E, H** and **I**) indicate staining near the centripetal pole, where the nucleus and lipid droplets (arrowheads in **A**, **D** and **G**) are also located. Images were not deconvolved. Scale bars are 50 $\mu$m.

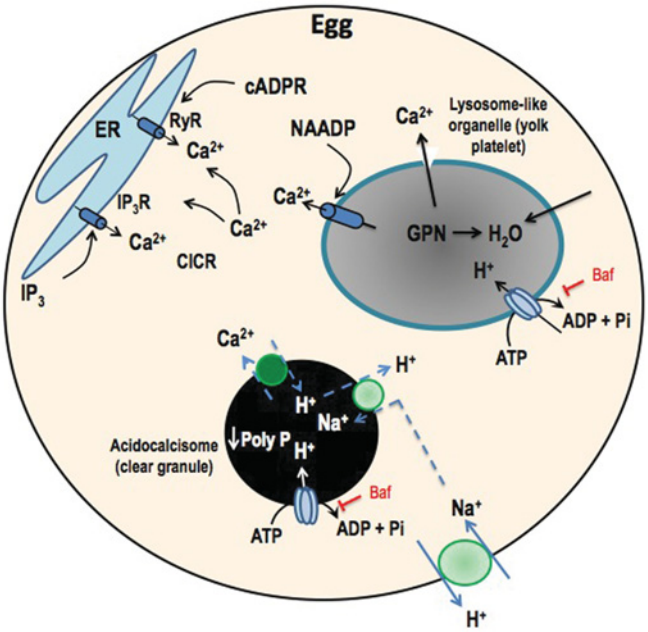


**Figure S3 Proposed $Ca^{2+}$ mobilization pathways in sea urchin eggs**

ER, acidocalcisomes and yolk platelets are major $Ca^{2+}$ storage organelles. $IP_3$ receptors ($IP_3R$) and ryanodine receptors (RyR) mediate $Ca^{2+}$ release from the ER in response to increases in $IP_3$ and cADPR respectively. Both receptors types are, in addition, activated by $Ca^{2+}$ via the so-called $Ca^{2+}$-induced $Ca^{2+}$-release mechanism (CICR). NAADP triggers $Ca^{2+}$ release from yolk platelets and this in turn triggers ER $Ca^{2+}$ mobilization through $Ca^{2+}$-induced $Ca^{2+}$ release via $IP_3R$ and RyR. $Na^+$ entry after fertilization leads to alkalinization of the cytosol and stimulates $Ca^{2+}$ release from acidocalcisomes by coupling the activity of $Na^+/H^+$ and $Ca^{2+}/H^+$ exchangers. GPN is hydrolysed by cathepsin C increasing the osmolarity of yolk platelets, attracting water and leading to osmotic lysis and $Ca^{2+}$ release. Both acidocalcisomes and yolk platelets possess bafilomycin $A_1$ (Baf)-sensitive vacuolar-type $H^+$-ATPases to acidify the organelles. Poly P is hydrolysed after alkalinization of acidocalcisomes.

Received 23 December 2009/6 May 2010; accepted 24 May 2010
Published as BJ Immediate Publication 24 May 2010, doi:10.1042/BJ20091956